G. K. Hu
Laboratoire MMS-MAT,
URA 850 CNRS Ecole Centrale Paris,
92295 Chatenay Malabry, France

F. Schmit
Centre de Recherche et d'Etudes
d'Arcueil ETCA,
16 bis Avenue Prier de la Cote d'Or,
94114 Arcueil, France

D. Baptiste

D. François

Laboratoire MMS-MAT,
URA 850 CNRS Ecole Central Paris,
92295 Chatenay Malabry, France

Viscoplastic Analysis of Adhesive Joints

The uniaxial constitutive law for an adhesive is studied by constant strain rate tensile, creep and relaxation tests. The S-D effect of the adhesive is taken into account by using the Raghava yielding criterion in a three dimensional constitutive formulation. The obtained constitutive law is then used to analyze a single lap joint and a butt joint by a finite element method. Constant cross head speed tensile and creep loading cases are examined. For a butt joint, the results show that the viscous effect and the influence of the hydrostatic stress must be taken into account due to the variation of the hydrostatic stress and of the loading rate in the adhesive layer as function of its thickness. A comparison with experimental results is also given. A good agreement between viscoplastic calculations and experimental results is obtained for single-lap joints. A reasonable result is obtained for butt joints and the discrepancy is attributed to interfacial debonding.

Introduction

Structural adhesives exhibit some sort of viscoelastic and viscoplastic behavior, especially ductile adhesives at high stress levels and at elevated temperatures. The redistribution of stress and strain in an adhesive joint during viscoelastic-viscoplastic deformation influences considerably the strength of the joints. In addition, adhesives usually exhibit different behavior in tension and in compression (S-D effect), which is associated with the important role of the hydrostatic stress in polymer yielding. In order to calculate more accurately the mechanical behavior of adhesive joints for engineering design, a more complete constitutive formulation for the mechanical behavior of adhesives is needed which accounts for these specific properties of polymeric materials.

The time-dependent behavior of adhesive joints has been studied by a number of investigators. Hayashi (1972) studied analytically the creep properties for a double lap joint. Delale and Erdogan (1981) used the Laplace transformation technique to study a single-lap joint with a viscoelastic adhesive. More recently, Groth (1990) studied viscoplastic stress in a single-lap joint using different rheological models. The S-D effect for adhesives was taken into account by Gali, Dolev, and Ishai (1981) and Raghava, Cadell, and Yeh (1975) for polymeric materials by introducing the influence of hydrostatic stress in the yield criteria. But it seems that little work has been conducted taking into account adhesive viscous and S-D effects for stress analysis in adhesive joints.

This paper presents a stress and strain analysis of adhesive joints using a viscoplastic adhesive model. The experimental study is performed on a commercial adhesive system Hysol EA9309.2. The uniaxial constitutive equation of the adhesive is investigated by constant strain rate, creep, and relaxation tests. The obtained uniaxial law is then generalized to three dimensions by using the Raghava yielding criterion (Raghava, Cadell, and Yeh, 1975), which takes into account the different behaviors of the adhesive in tension and compression. The obtained constitutive model for the adhesive is used for finite element analysis. The calculated results are then compared with experimental values.

Mechanical Behavior of Bulk Adhesive

The Hysol EA 9309.2 adhesive used in our analysis is a two constituent epoxy system which can be cured at room temperature. To obtain short-term stable mechanical properties, the adhesive was cured for one week at room temperature and post-cured for three days at 50°C.

The uniaxial tensile behavior of the bulk adhesive is determined by using standard ISO 1/2 specimens fabricated from a 1mm plate of hardened adhesive in accordance with NFT91-034 standards.

The mechanical tests, consisting of constant strain-rate tensile, short-term creep, and relaxation tests, are performed at room temperature with a computer controlled testing machine. The strain is measured by a slip gage extensometer. The experimental results are presented in Figs. 1(a) and 1(b), 2 and 3.

These experimental results, as well as loading and unloading tests (Hu, 1991), show that the viscoplastic deformation of the adhesive is very important and that the adhesive displays little strain hardening (Fig. 2). The creep tests (Fig. 1(b)) show that the creep strain is negligible at low stress levels; but at high stress levels, the three stages of creep (primary, secondary, and tertiary) occur. The secondary creep stage dominates most of the adhesive creep life. Therefore, in the following model, only the secondary creep is taken into account. A creep threshold of $\theta = 20$ MPa, based on the creep tests, is proposed, below which the creep strain is neglected.

Based on these considerations, a Norton-type (Lemaitre and Chaboche, 1988) viscoplastic law is used in a uniaxial formulation:

$$\dot{\epsilon} = \left(\frac{\sigma - \theta}{\mu}\right)^k \quad (1)$$

where $\dot{\epsilon}$ is the creep rate at an applied stress σ. μ, k are material constants, which are derived from the creep and the constant strain rate tension tests, giving

$$\mu = 54 \text{ MPa}, \quad k = 8.99.$$

As shown in Figs. 1–3, the uniaxial model can describe well

Contributed by the Applied Mechanics Division of THE AMERICAN SOCIETY OF MECHANICAL ENGINEERS for publication in the ASME JOURNAL OF APPLIED MECHANICS.

Discussion on this paper should be addressed to the Technical Editor, Professor Lewis T. Wheeler, Department of Mechanical Engineering, University of Houston, Houston, TX 77204-4792, and will be accepted until four months after final publication of the paper itself in the ASME JOURNAL OF APPLIED MECHANICS.

Manuscript received by the ASME Applied Mechanics Division, July 26, 1991; final revision, Feb. 16, 1992. Associate Technical Editor: J. W. Rudnicki.

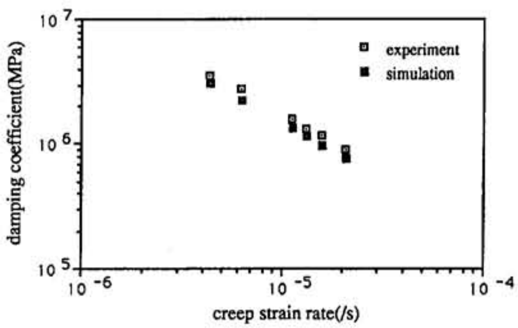

Fig. 1(*a*) Simulational and experimental creep tests for the bulk adhesive

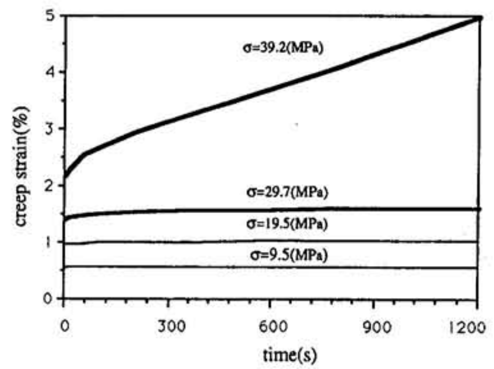

Fig. 1(*b*) Creep tests for the bulk adhesive

the experimental results for the bulk adhesive (the damping coefficient is defined as $\beta = (\sigma - \theta)/\dot{\varepsilon}$). For the relaxation case, it is seen that at lower applied strain levels, there is a difference between the experimental and the calculated curves. This difference comes from the fact that at lower applied strain levels, the primary creep is very important, which is not taken into account in our model.

In the sections which follow, this uniaxial equation is used as the basis for a three-dimensional constitutive formulation.

Three-Dimensional Formulation

In order to analyze the stress distribution in adhesive joints, a three-dimensional constitutive formulation for adhesives is necessary. In our study, the method outlined by Betten (1989) is used and an equivalent stress from the Raghava criterion (Raghava, Cadell, and Yeh, 1975) is proposed to account for the different behaviors of adhesives in tension and compression.

For creep mechanics, the constitutive equation can be written in a general form,

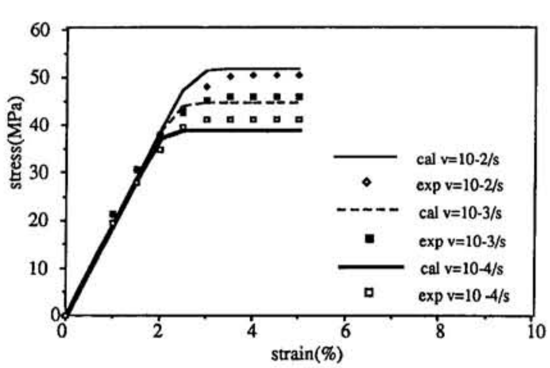

Fig. 2 Simulational and experimental constant strain rate tensile tests

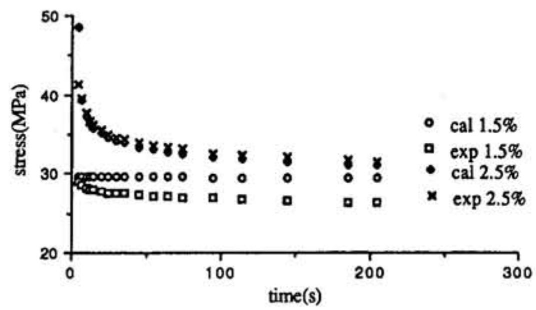

Fig. 3 Simulational and experimental relaxation tests

$$\dot{\boldsymbol{\epsilon}} = \mathbf{f}(\boldsymbol{\sigma}, \boldsymbol{\omega}, \mathbf{A}) \tag{2}$$

where $\boldsymbol{\sigma}$ is the applied stress tensor, $\boldsymbol{\omega}$ the damage tensor, $\mathbf{A}$ the tensor of anisotropy, and $\dot{\boldsymbol{\epsilon}}$ the creep strain rate tensor.

In our case, the anisotropy and the damage of the adhesive are neglected; furthermore the nonlinear stress tensor terms are also neglected for simplification. Under these conditions, Eq. (2) yields:

$$\dot{\boldsymbol{\epsilon}} = \varphi_0 \mathbf{I} + \varphi_1 \mathbf{s} \tag{3}$$

where φ_0 and φ_1 are two scalar coefficients depending only on the experimental data and the stress invariant, $\mathbf{s}$ is the deviatoric part of stress tensor $\boldsymbol{\sigma}$; and $\mathbf{I}$ is the unit tensor. φ_0 and φ_1 are identified from Eqs. (3) and (1), giving:

$$\varphi_0 = \frac{1 - 2\nu}{3\mu^k} (\sigma - \theta)^k \tag{4}$$

$$\varphi_1 = \frac{(1 + \nu)}{\mu^k} \frac{(\sigma - \theta)^k}{\sigma} \tag{5}$$

where ν is the Poisson's ratio and σ is an equivalent stress. In our case, to take into account the S-D effect of the adhesive, an equivalent stress other than that of Von Mises should be defined. For polymeric materials, the Raghava yielding criterion is widely used:

$$J_{2d}^2 + (\sigma_c - \sigma_t) I = \sigma_c \sigma_t \tag{6}$$

with

$$J_{2d} = (1.5 s_{ij} s_{ij})^{0.5} \tag{7}$$

$$I = \sigma_{ii} \tag{8}$$

where σ_c and σ_t are the elastic limits in compression and in tension, respectively. From this yielding criterion, the equivalent stress is obtained:

$$\sigma_{eq} = \frac{I(\lambda - 1) + (I^2(\lambda - 1)^2 + 4 J_{2d}^2 \lambda)^{0.5}}{2\lambda} \tag{9}$$

where λ is defined as σ_c/σ_t.

The general constitutive equation can then be derived from Eqs. (3), (4), (5) and (9):

$$\dot{\boldsymbol{\epsilon}} = \frac{(1 - 2\nu)}{3\mu^k} (\sigma_{eq} - \theta)^k \mathbf{I} + \frac{(1 + \nu)}{\mu^k} (\sigma_{eq} - \theta)^k \frac{\mathbf{s}}{\sigma_{eq}}. \tag{10}$$

From Eq. (10), it is found that the Norton constitutive equation is a special case in which incompressibility and the Von Mises equivalent stress are assumed.

This constitutive equation is implemented into the finite element code ZEBULON (Burlet and Cailletaud, 1991). This finite element code is capable of performing linear and nonlinear, static, and dynamic analyses. The Poisson's ratio is a function of deformation, and here, for simplification, we chose $\nu_c = 0.5$ when the adhesive is plastic. λ is taken to be 1.2, as is commonly

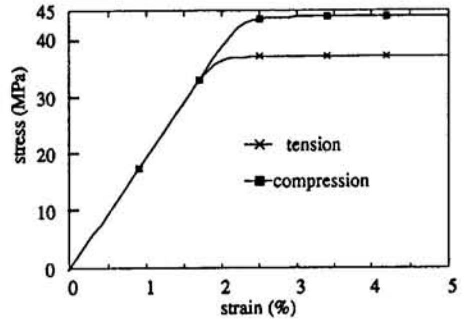

Fig. 4 Calculated tension and compression stress-strain curves at a strain rate 10^{-4}/s for the bulk adhesive

used for polymeric materials (Adams and Wake, 1984). The uniaxial curves in tension and compression for the adhesive are calculated at a strain rate of $10^{-4}\ s^{-1}$ (see Fig. 4) in order to check the finite element code. The result shows that the present constitutive model can reflect the different behaviors of the adhesive in tension and in compression. This constitutive relation is then used to analyze the stress distribution in adhesive joints.

Viscoplastic Stress Analysis of Adhesive Joints

In the following section, a single-lap joint in creep and a butt joint in constant cross head speed tension tests are examined with emphasis on viscous and S-D effect on adhesive joints. The adherent is an aluminium alloy with mechanical constants $E_s = 73000$ MPa, $\nu_s = 0.29$, and the elastic constants for the adhesive are $E_c = 1950$ MPa, $\nu_c = 0.36$.

Single Lap Joint in Creep. The finite element mesh of a single-lap joint is shown in Fig. 5 (the adhesive thickness is 0.5mm). The elements are two-dimensional, eight-node, quadratic elements which can be used for plane-stress, plane-strain, and axisymmetric problems. Geometrical nonlinearity was not included, thus limiting the analysis to material nonlinearity with small displacements. The boundary conditions are shown in Fig. 5. A pressure corresponding to an average shear stress of approximately 20 MPa is applied for a short time, and then it is kept constant on the line AA′ (Fig. 5). The calculation is performed under a plane-strain condition.

The distribution of the shear stress and normal stress in the joint at the mid line ($x1$) (Fig. 5) is shown in Figs. 6(a) and

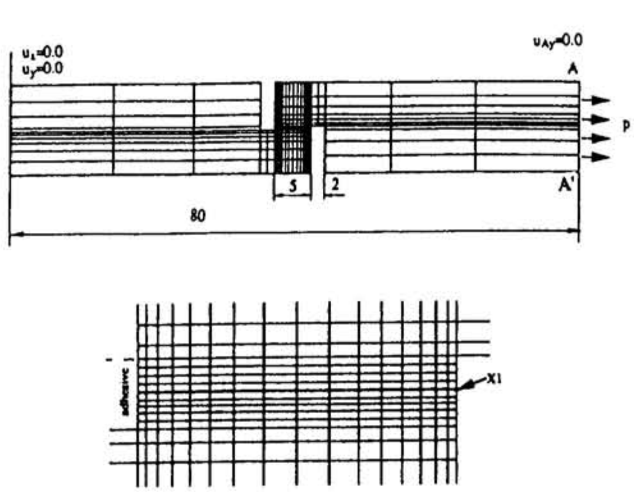

Fig. 5 Finite element analysis of a single-lap joint

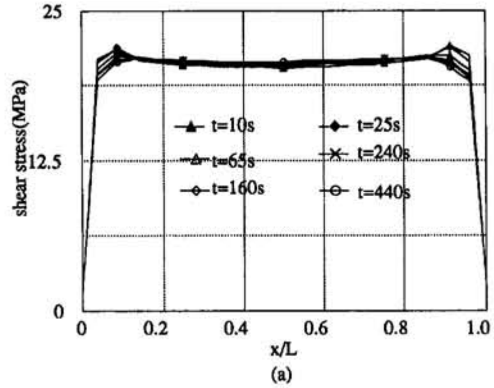

Fig. 6(a) Creep shear stress distribution along the mid-line of single-lap joint

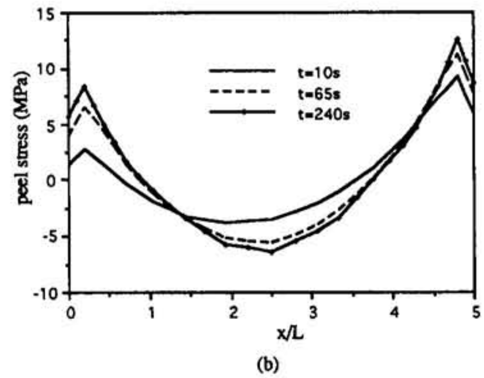

Fig. 6(b) Creep normal stress along the mid-line of single-lap joint

6(b). The shear stress concentration at the joint ends is relaxed by creep. The shear stress tends to be homogeneously redistributed along the joint due to the viscosity of the adhesive. By contrast, the normal stress has a tendancy to increase at the joint ends. The asymmetry of the peel stress is due to a small rotation of the applied force line arising from the asymmetry of the joint.

The displacement at the middle of line AA′ as a function of time is plotted in Fig. 7. At this loading level, the displacement of the joints continues to increase and creep fracture is unavoidable. This loading level is therefore unacceptable for engineering design. The relaxed shear stress is compensated in the middle of the joint, enhancing the stress level there (Fig. 6(b)). Thus the shear stress (minimum stress) at the midpoint of the joint should always be kept at a value less than the creep limit to avoid creep failure. This is contrary to the ultimate joint strength that is governed by the maximum stress or strain as

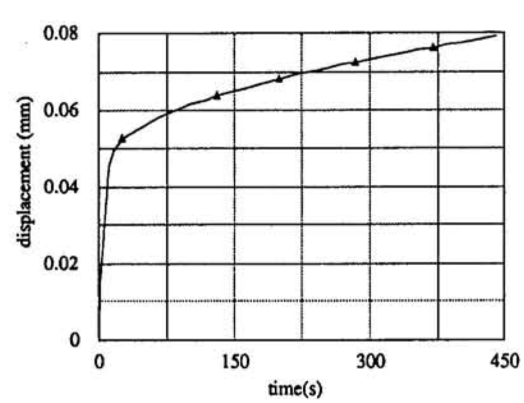

Fig. 7 Displacement evolution as a function of creep time

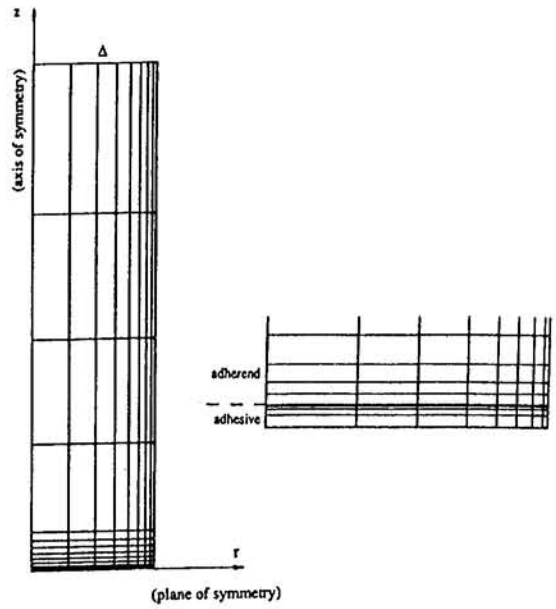

Fig. 8 Finite element analysis of a butt joint

proposed by Hart-Smith (1981). This viscoplastic model can provide a useful tool for creep design of adhesive joints and for studying the viscous influence of adhesive joints.

Butt Joint in Tension. In order to investigate the S-D effect in adhesive joints, a butt joint is examined by a finite element method using the obtained constitutive adhesive model. This kind of joint has been examined by many authors. Adams et al. (1978) studied the elastic case for this type of joint by finite element method; Anderson and DeVries (1989) used fracture mechanics to evaluate the joint strength. This kind of joint is particularly interesting for our analysis. If the cross head speed is kept constant, the loading rate and hydrostatic stress of the adhesive layer changes with varying thickness. These two factors determine the mechanical behavior of the adhesive layer.

In our analysis, the butt joint consists of two aluminum alloy cylinders bonded with the same adhesive as before. Mechanical behavior is investigated both by a finite element analysis and experimentally. The finite element mesh is shown in Fig. 8. Due to the symmetry, only a quarter of the joint is analyzed. The thickness of the adhesive layer is chosen as 0.5mm with a cylinder diameter of 10mm. A displacement of 0.08mm is applied for 13 seconds, corresponding to a cross head speed of 5 $\times 10^{-3}$mm/s.

The axial and radial stress distributions are shown at the midplane of the adhesive in Figs. 9(*a*) and (*b*). There is little variation in the axial stress σ_{zz} during loading when the adhesive begins to deform plastically. This stress remains almost constant in the joint except near the ends, which are perturbed by the edge singularity. In the central region, the axial stress is slightly higher than the average applied stress needed to satisfy the equilibrium condition. But σ_{rr} decreases with increasing loading. An important hydrostatic stress is induced in the joint due to the difference in Poisson's ratios between the adherents and the adhesive. This stress varies in the same manner as σ_{rr} and it reaches about 28 MPa. The zone influenced by the edge singularity decreases with decreasing adhesive thickness.

The average stress-strain relation of the adhesive layer is also studied as a function of its thickness (see Fig. 10). All of the calculations are performed at the same cross-head speed of 5 $\times 10^{-3}$mm/s. The results show that the tensile stiffness of a butt joint decreases with increasing adhesive thickness due to the diminution of the hydrostatic stress in the adhesive layer (Fig. 11). The variation of the maximum stress in the adhesive

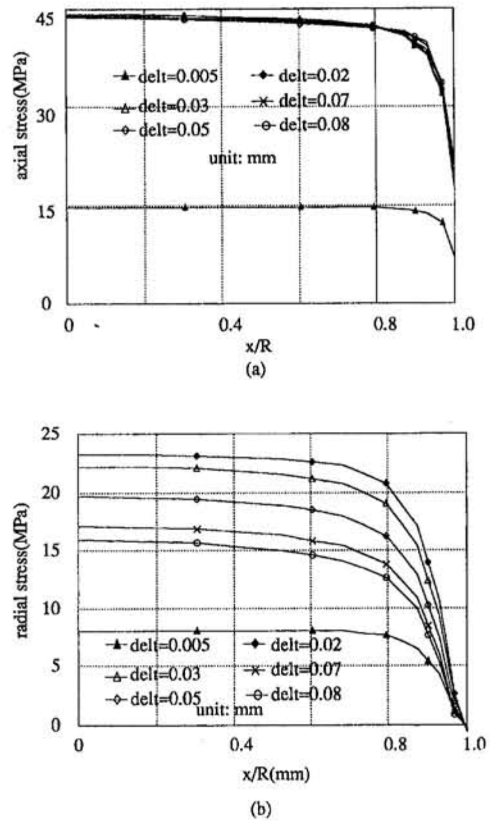

Fig. 9(*a*) Axial stress distribution along the mid-line of butt joint; (*b*) radial stress distribution along the mid-line of butt joint

layer is shown in Fig. 11. For a joint with adhesive thickness of 0.1, 0.3, and 0.5 mm, there is very little variation of the maximum stress (this is confirmed experimentally). For the joint with a 3mm thickness, there is an increase of the maximum stress and this stress decreases when the adhesive thickness is further increased. Finally, the behavior of the bulk adhesive dominates for very large adhesive thicknesses (approximately the diameter of adherent).

This variation comes from competition between the tensile loading rate of the adhesive layer and the hydrostatic stress state as a function of the adhesive thickness during a constant cross-head speed test. In fact, for thinner adhesive thicknesses, the loading rate of the adhesive layer increases and the viscosity has little time to manifest itself. But because the hydrostatic stress is higher, a high equivalent stress (as defined previously) is induced, and it increases the relaxation rate. For the adhesive

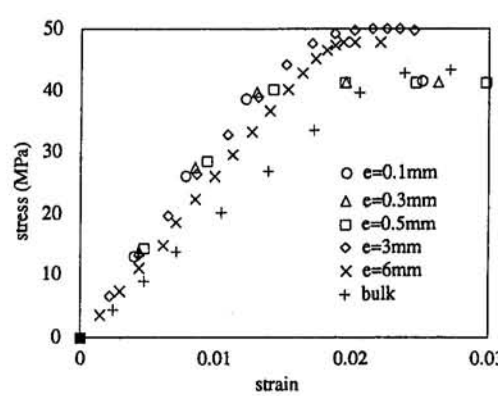

Fig. 10 Average stress and strain relations of adhesive layer as a function of adhesive thickness in a butt joint

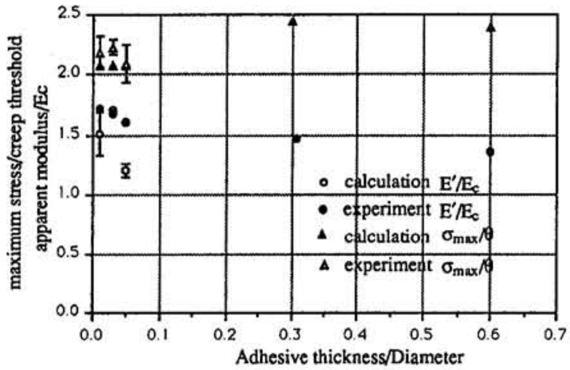

Fig. 11 Butt joint stiffness and maximum average axial stress variations as a function of adhesive thickness

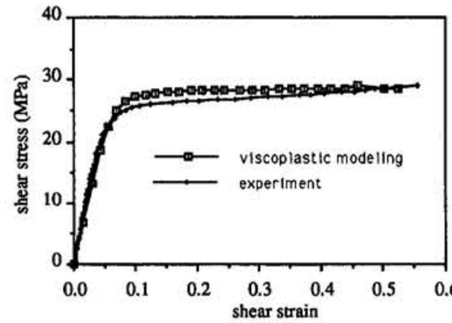

Fig. 12 Comparison between the model and experimental results of a single-lap joint

layer of 3mm, the influence of the hydrostatic stress is trivial, and the adhesive behavior is determined mainly by the increasing loading rate.

The variation of the loading rate in the adhesive layers can be estimated. If E_s and l_s represent the Young's modulus and the length of the adherent, respectively, and E_c and l_c those of the adhesive, the total elongation of the adhesive joint (Δl) can be calculated:

$$\begin{aligned}\Delta l &= \Delta l_s + \Delta l_c \\ &= \epsilon_s l_s + \epsilon_c l_c \end{aligned} \tag{11}$$

so that the average deformation rate of the joint is given by:

$$\dot{\delta} = \frac{\Delta l}{l} = \frac{\dot{\epsilon}_s l_s}{l} + \frac{\dot{\epsilon}_c l_c}{l} \tag{12}$$

where ϵ_s and ϵ_c are the average strains in the adherents and the adhesive respectively; $\dot{\epsilon}_s$ and $\dot{\epsilon}_c$ denote the average strain rates in the adherents and the adhesive, respectively; $\dot{\delta}$ is the transverse loading rate and l denotes the total joint length.

In the elastic case, the following relation between the strain rate in the adherent and in the adhesive is available:

$$\frac{\dot{\epsilon}_c}{\dot{\epsilon}_s} = \frac{E_s}{E_c}. \tag{13}$$

With Eqs. (12) and (13) the strain rate can then be determined.

In the plastic case, the strain rate in the adherent is taken to be zero since the stress variation in the adherent is almost negligible, and the strain rate in the adhesive layer is calculated by Eq. (12).

For a butt joint having a total joint length of 40mm and an adhesive thickness of 0.5mm, the variation of the loading rate in the adhesive can be three times greater than that initially. When the adhesive is completely plastic, the loading rate is 80 times that of the average loading rate in the joint.

Experimental Comparison

The experimental comparison is performed on both single lap and butt joints at constant cross-head speed loading. The individual specimens are cut and machined from aluminium alloy plates bonded with the adhesive. The cure condition used for the bulk adhesive previously described is adopted. Before bonding, the 2024 T6 aluminium adherents were surface treated with a chromic acid etch to prepare the surfaces.

The tensile tests, using a cross head speed of 1mm/min, are carried out for single lap joints. The average shear strain is measured by an ALTHOF extensometer (Hu, 1991), and the average shear stress is calculated by dividing the applied load by the bonded surface area. The adhesive thickness here is 0.5mm. The comparitive result is shown in Fig. 12. A good agreement between the experimental results and the model is obtained.

For butt joints, the mechanical tests are performed at a cross head speed of 5×10^{-3}mm/s. The displacement of the adhesive layer is measured by a slip gage extensometer. The average strain is calculated as being the ratio of the displacement of the adhesive layer to its thickness; the displacement of the adhesive layer is calculated by removing that owing to the adherents from the value measured by the extensometer. The experimental results are compared with the viscoplastic finite element analysis (Fig. 13). A reasonable agreement is also obtained between the model and the experiments. The small discrepancy undoubtedly comes from interfacial debonding that is unaccounted for in the model, but observed in adhesive joints tested in tension within a scanning electron microscope (Hu, 1991). For single-lap joints, only very little localized debonding occured.

Conclusion

The general constitutive relation of an adhesive was studied experimentally and theoretically to take into account the viscosity and the influence of the hydrostatic stress. The calculated results for adhesive joints using the obtained constitutive equation show that for a single-lap joint under a creep load, the shear stress concentration is relaxed by creep. The relaxed shear stress is compensated by an enhanced shear stress in the centeral region of the joint. This stress level should always be kept under than the creep limit to prevent creep failure of the joints. For a butt joint subjected to a constant cross-head speed loading, the hydrostatic stress and the loading rate in the adhesive layer varies as a function of the adhesive thickness. The competition between these two factors with varying adhesive thickness is taken into account in the present analyzes. The results show that for thinner joints, the stiffness is more important and the maximum stress varies little (0.1mm to 0.5mm). By increasing the joint thickness, the influence of the hydrostatic stress de-

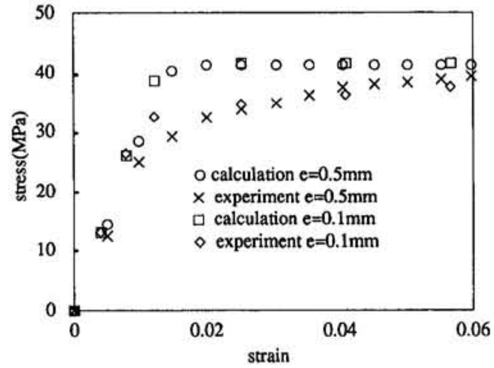

Fig. 13 Comparison between the model and experiment of a butt joint

creases and the influence of the loading rate dominates the behavior. This leads to an increase in the maximum stress in the joint. Finally for very large joint thicknesses (approximately equal to the cylinder diameter), the adhesive bulk material properties are exhibited. The experimental result shows a good agreement with our analyzes for single-lap joints, and a reasonable result is obtained for butt joints. The difference between the model and the experiments for butt joints is probably due to interfacial debonding which is not taken into account in present model.

References

Adams, R. D., Coppendale, J., and Peppiatt, N. A., 1978, "Stress Analysis of Axisymmetric Butt Joints Loaded in Torsion and Tension," *J. of Strain Analysis*, Vol. 13, No. 1, pp. 1–10.

Adams, R. D., and Wake, W. C., 1984, *Structural Adhesive Joints in Engineering*, Elsevier, New York.

Anderson, G. P., and DeVries, K. L., 1989, "Predicting Strength of Adhesive Joints From Test Results," *Int. J. of Fracture*, Vol. 39, pp. 191–200.

Betten, J., 1989, "Generalization of Nonlinear Materials Laws Found in Experiments to Multi-axial States of Stress," *Eur. J. Mech.*, A/solids 8, No. 5, pp. 325–339.

Burlet, H., and Cailletaud, G., 1991, "ZEBULON, A Finite Element Code for Nonlinear Materials Behavior," Eur. Conference on New Advances in Computational Structural Mechanics, Apr. 2–5, Giens, France.

Delale, F., and Erdogan, F., 1981, "Viscoelastic Analysis of Adhesively Bonded Joints," ASME JOURNAL OF APPLIED MECHANICS, Vol. 48, pp. 331–338.

Gali, S., Dolev, G., and Ishai, O., 1981, "An Effective Stress/Strain Concept in the Mechanical Characterization of Structural Adhesive Bonding," *Int. J. Adhesion and Adhesive*, Jan., pp. 135–140.

Groth, H. L., 1990, "Viscoelastic and Viscoplastic Stress Analysis of Adhesive Joint," *Int. J. Adhesion and Adhesive*, Vol. 10, pp. 207–213.

Lemaitre, J., and Chaboche, J. L., 1988, "Mécanique des Matériaux Solides," Dunod.

Hart-Smith, L. J., 1981, "Stress Analysis: A Continuum Mechanics Approach," *Developments in Adhesives-2*, Kinloch, ed., Applied Science Publishers, LTD, pp. 1–45.

Hayashi, T., 1972, "Creep Analysis of Bonded Joints," *Composite, Mater. and Structure*, Vol. 1, No. 2, pp. 58–63.

Hu, G. K., 1991, "Approche Théorique et Expérimentale du Comportement Mécanique, de l'Endommagement et de la Rupture des Assemblages Collées," Ph.D, Ecole Centrale Paris.

Raghava, R. S., Cadell, R. M., and Yeh, G. S. V., 1975, "The Macroscopic Yield Behavior of Polymers," ASME JOURNAL OF APPLIED MECHANICS, Vol. 8, pp. 225–232.